Nima Norouzi[1,2], Zahra Nouri[3, *]

[1]School of Medicine, Queen Mary University of London, Mile End Road, London E1 4NS, London, UK

[2]School of Medicine, Queen Mary University of London, Mile End Road, London E1 4NS, London, UK

[3]School of Medicine, Tehran University of medical science, Tehran, Iran

Simulation of erythrocyte deformation and drug delivery using the Boltzmann network method

***Abstract*—** In this paper, a combination of the Boltzmann network method and the immersion boundary simulates the behavior and deformation of erythrocytes with different primary shapes. Initially, erythrocytes were simulated with an elliptical geometry in a shear flow, and the deformation obtained was compared with the results of other researchers. Then, different geometries of red blood cells in shear flow and during their movement and displacement, simulation, and their gradual deformation have been observed and analyzed. In the following, the flow of fluid inside a blood vessel is modeled, and with its help, phenomena such as blockage of the blood vessel and drug delivery are studied. The results show that damage to the artery wall or deposition of fat masses will cause vortex blood flow and blood clot formation. Also, the quality of drug injection in this two-pronged artery is very influential in how it is delivered. Finally, comparing the results with the results of others shows that this simulation has acceptable accuracy.

Received 19 May 2021.
Revised 26 June 2021.
Accepted 26 June 2021.
Published Online 30 June 2021

*Corresponding author:
Nima Norouzi
Email: n.nima1376@gmail.com

***Keywords*—Red blood cell, Boltzmann network method, Immersion boundary, Blood vessel occlusion, Drug delivery.**

1 INTRODUCTION

The main purpose of this paper is to simulate the behavior of red blood cells as well as complex currents in vascular pathways such as the carotid artery and drug delivery analysis in this artery. Recently, a combination of the Boltzmann lattice method with the immersion boundary method has been used to simulate the movement and deformation of red blood cells. The immersion boundary method has been successfully used in recent decades to simulate the elastic and flexible dynamics of immersion in the fluid. This method was first introduced by Peskin [1] to study the flow around the heart valve and later expanded as an efficient method in solving problems related to fluid-solid interaction. This method is a combination of mathematical formulation and numerical methods. The mathematical formulation of the immersive boundary method includes the Eulerian and Lagrangian variables related to the Dirac delta function. In the discretization of the equations related to the immersion boundary method, a Cartesian network is used for Eulerian variables, and a linear curve network for Lagrangian variables is used. The curvilinear grid can move freely within the Cartesian grid and does not need to adapt to the Eulerian grid. In the present study, the deformation of erythrocytes and how they are delivered in a blood vessel are studied using a combination of the Boltzmann network method and the immersion boundary. The Boltzmann lattice method (LBM) is a robust numerical technique based on kinetic theory for fluid field simulation [2-5]. Compared to conventional computational fluid dynamics methods, the advantages of using the Boltzmann lattice method include simple calculation method, simple execution, and use of Simple techniques in the analysis of complex geometries are the Boltzmann equations, resulting in a discretization $f_i(x,t) = f(x,c,t)$ that describes the probability of the existence of a particle in a lattice with position x at time t. While moving at a speed of ci, according to the conventional numerical methods commonly used to study fluid behavior, the kinetic nature of the Boltzmann lattice involves easy implementation in complex boundary conditions. In addition, in the macroscopic method of computational fluid dynamics, The pressure field is usually calculated by solving Poisson equations obtained from the Navier-Stokes incompressible

equation, which is usually time-consuming. In contrast, the pressure distribution can be easily calculated in the Boltzmann lattice method by solving a simple state equation. In addition, the conversion of mesoscopic values of the distribution function to macro parameters The scope is a simple mathematical process. Blood flow simulations have also been considered in previous studies. Quiza et al. [6] have proposed a multidimensional model for studying blood flow using the finite element method. Butner et al. [7] have proposed a three-dimensional model to simulate the developed flow within blood vessels. Deschamps et al. [8] directly modeled blood flow within a vessel without creating additional networks and complex details. In the present study, the methods presented in references [9 and 10] were used to simulate the curved vessel wall, and neohookin relations were used to calculate the shear stress on the viscoelastic wall erythrocyte cell membrane. Finally, the simulation results have been compared to the results obtained from previous studies.

2 MATH

Particle kinetic theory, especially the Boltzmann lattice method, has been significantly developed to analyze different numerical simulation problems [11-13]. The Boltzmann lattice method is inferred from the gas lattice method and the discretization of the Boltzmann equation. This method is a powerful numerical technique for simulating fluid flow [11, 14, 15], heat transfer [17, 16], and various other applications than traditional computational fluid dynamics methods. Unlike the classical Navier-Stokes macroscopic approach, the mesoscopic model uses fluid flow simulation [16]. This method uses fluid particle motion modeling to achieve macroscopic fluid properties such as velocity and pressure. In this method, the fluid field is discretized into Cartesian uniform cells, and each cell is assigned a constant amount of distribution function that represents the number of fluid particles moving in the direction of the discrete directions. Different models have been presented based on the number of dimensions studied and the number of speed directions. This paper is based on a two-dimensional Boltzmann network with nine directional velocities (D2Q9). The velocity directions in a D2Q9 model are shown in Fig. 1,

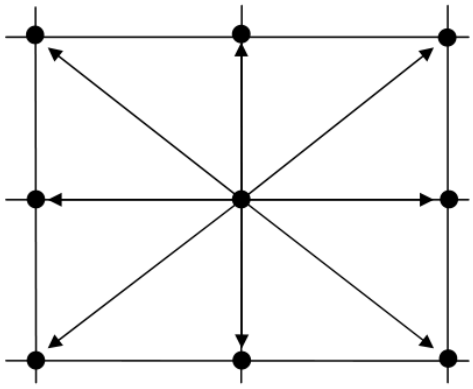

Figure 1: Boltzmann D2Q9 model of the network

and the velocities shown are as follows, where c =Δx⁄Δt and K represents the velocity vectors.

$$c_k = \begin{cases} (0,0) & k = 0 \\ (\pm 1,0)c, (0,\pm 1)c & k = 1,2,3,4 \\ (\pm 1,\pm 1)c & k = 5,6,7,8 \end{cases} \quad (1)$$

The model used in this article is the same model mentioned other studies [16]. The distribution function is computed by solving the Boltzmann equation, which results from a special discretization of the Boltzmann kinetic equation. Following the Bhatnagar-Gross-Krook approximation, the Boltzmann equation is formulated as follows:

$$f_k(x + c_k\Delta t, t + \Delta t) = f_k(x,t) + \frac{\Delta t}{\tau}\left[f_k^{eq}(x,t) - f_k(x,t)\right] + \Delta t c_k F_k \quad (2)$$

Where Δt represents the time step, c_k is the discrete speed of the network in the direction of k, τ is the time of comfort of the network, f_k^{eq} is the function of the equilibrium distribution and F_k is the external force applied in different directions of the network speed.

The equilibrium distribution function mentioned in equation (2) is calculated as follows:

$$f_k^{eq} = \omega_k \rho \left[1 + \frac{c_k.u}{c_s^2} + \frac{1}{2}\frac{(c_k.u)^2}{c_s^4} - \frac{1}{2}\frac{u^2}{c_s^2}\right] \quad (3)$$

Where for k = 0 weight ω_k= 4/9, for k = 1,2,3,4 weight ω_k = 1/9, k = 5,6,7,8 weight ω_k = 1/36 and also c_s = $c_k/\sqrt{3}$ is macro values of fluid such as density and velocity are calculated as follows:

$$\rho = \sum_{k=0}^{8} f_k, u = \frac{1}{\rho}\sum_{k=0}^{8} f_k c_k \quad (4)$$

2.1 Curve boundary conditions

According to Fig. 2, it can be seen that the black circle x_w corresponds to the curve boundary, the hollow circle x_f corresponds to the points of the fluid field, and the gray circle x_b Corresponds to the solid points. To apply the streaming phase on the boundary, we need to calculate $\tilde{f}$ $(x_{b,t})$, the next distance between the points in the fluid field and the boundary of the curve is calculated as follows:

$$\Delta = \frac{\|x_f - x_w\|}{\|x_f - x_b\|} \quad (5)$$

Fig. 3 shows three models of solid boundary placement in a network. Figure 3a shows a typical solid boundary in which the boundary is exactly in the middle of the fluid and solid field, in which case $\Delta = 0.5$ is considered. Figures 3b and 3c show conditions in which the value is less than

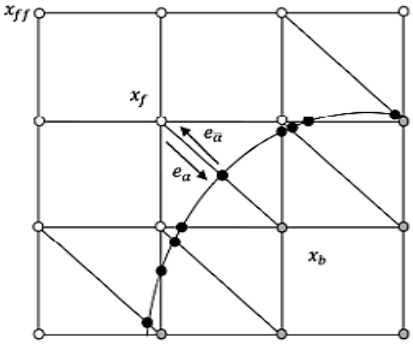

Figure 2: Schematic view of a Cartesian grid and curved border

or greater than 0.5. In all three cases, the value of the reflected distribution function $f_a(x,t+\Delta t)$ is unknown.

To calculate this value in the node x_f intermediate must be used. The method used to calculate the velocity field in the face of the curved boundary of the method used in this project is similar to the method proposed in other studies [18]. To calculate the distribution function in the solid part $f_a(x_{b,t})$ based on the boundary nodes located in the fluid field, the solid boundary conditions are used considering the distance between the fluid node and the boundary. The Chapman-Anscog model for calculating the collision phase distribution function is as follows:

$$\tilde{f}_{\bar{\alpha}}(x_b, t+\Delta t) = (1-\lambda)\tilde{f}_{\alpha}(x_f, t+\Delta t) + \lambda f_{\alpha}^{0}(x_b, t+\Delta t) - 2\frac{3}{c^2} w_\alpha \rho(x_f, t+\Delta t) e_\alpha . u_w \quad (6)$$

$$f_{\alpha}^{0}(x_b, t+\Delta t) = f_{\alpha}^{eq}(x_f, t+\Delta t) + \frac{3}{c^2} w_\alpha \rho(x_f, t+\Delta t) e_\alpha (u_{bf} - u_f) \quad (7)$$

$$u_{bf} = u_{ff}, \lambda = \frac{2\Delta - 1}{\tau_m - 2} \qquad if\ 0 < \Delta \leq \frac{1}{2} \quad (8a)$$

$$u_{bf} = \left(1 - \frac{3}{2\Delta}\right) u_f + \frac{3}{2\Delta} u_w, \lambda = \frac{2\Delta - 1}{\tau_m + \frac{1}{2}} \qquad if\ \frac{1}{2} < \Delta \leq 1 \quad (8b)$$

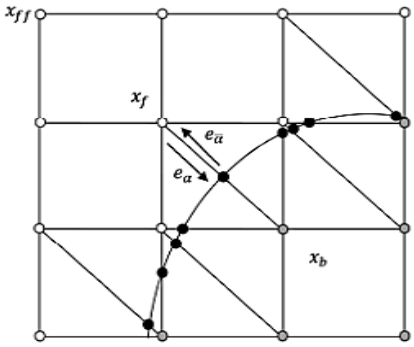

Figure 3: Solid-State boundary image in the Boltzmann Lattice

2.2 Immersion border

The submerged boundary method is derived from the principle that deformation and movement of the boundary create a force that tends to return the boundary to its original shape or location. The connection between the membrane and the surrounding fluid is achieved by distributing local membrane and fluid forces. To satisfy the no-slip condition, the velocity in the membrane and the surrounding fluid must be the same, so the local fluid force sentence is calculated as follows:

$$F_k = \left(\frac{1}{1-2\tau}\right)\omega_k \left[\frac{(u_k - u)}{c_s^2} + \frac{(c_k . u)}{c_s^4} c_k\right] f \quad (9)$$

The relationship between the immersion boundary and the fluid flow by the membrane force is as follows [19],

$$f(x,t) = \int_{\Gamma} F(s,t)\delta(x - X(s,t))ds \quad (10)$$

Where f is the force density, F is the membrane force, and s are the followers of the immersion boundary nodes. The structural model used for cell membranes in this paper is the Neo-Hawkin equation, which has a strain energy function as:

$$W^{NH} = E(\varepsilon_1^2 + \varepsilon_2^2 + \varepsilon_1^{-2}\varepsilon_1^{-2}) \quad (11)$$

For erythrocytes, the stress along the membrane is calculated as follows

$$T = \frac{E}{\varepsilon^{3/2}}(\varepsilon^3 - 1); \varepsilon_1 = \varepsilon_2 \quad (12)$$

Finally, the membrane force, which is the result of the stress of adjacent nodes (j, i) and is calculated as follows:

$$F = T_i e_i - T_j e_j \quad (13)$$

2.3 Validation of results

To simulate erythrocytes in shear flow, the values of different parameters are determined according to Table 1. The most important property of the flow between two parallel plates is that the shear stress of the fluid remains constant. In other words, the velocity changes concerning the distance between two plane lines. For this purpose, to determine the accuracy of the simulation of velocity changes between two plates for different values of comfort time has been investigated (Figure 4). As can be seen, the comfort time τ = 0.6 had the closest profile to the linear profile used in this simulation.

Table I: Dimensional parameters and values

Parameter	Value
Cell radius	$6\ \mu m$
Channel diameter	$12\ \mu m$
Shear modulus of elasticity (E_s)	$1.2\times10^{-3}\ dyn/cm$
Shear rate (γ˙)	$4.2\ s^{-1}$
Re	1.26×10^{-4}
$\mu_p = 1.2\ c_p$	$\mu_c = 6\ cp$
$\lambda = \frac{\mu_c}{\mu_p}$	5

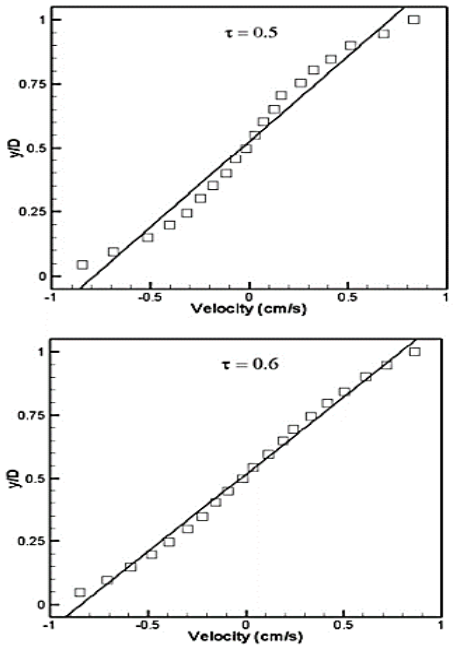

Figure 4: Speed profile between two parallel plates for different values of comfort line

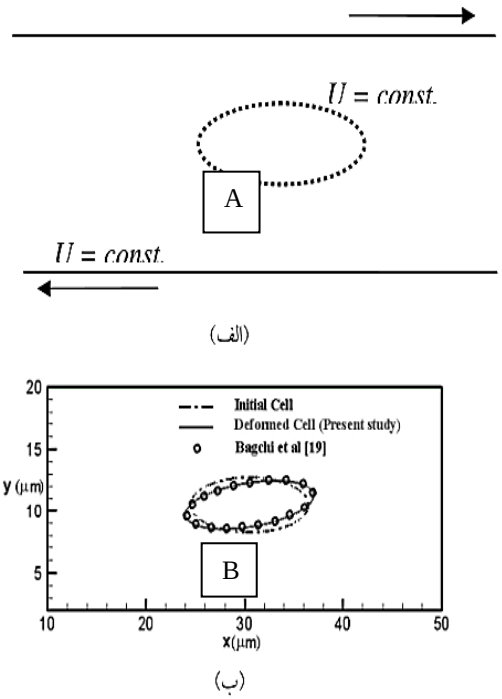

Figure 5: (A) Physical model (B) Elliptical cell deformation

Next, the deformation of an erythrocyte ellipse cell is examined. As shown in Fig. 5-a, the red blood cells move at constant and opposite velocities in the center of the canal and the upper and lower walls. Fig. 5-b shows the results of the deformation of an elliptical cell, which is in good agreement with the results presented by Begchi et al. [19].

$$\bar{y} = 0.5(1-\bar{x}^2)^{0.5}(c_0 + c_1\bar{x}^2 + c_2\bar{x}^4)$$
$$-1 \le \bar{x} \le 1;\ c_0 = 0.207, c_1 = 2.002, c_2 = 1.122$$

3 Results and Discussion

In the previous section, the original shape of the cell was assumed to be oval, and its deformation was compared with Bagchi's results. However, the actual shape of the cell is in the form of two biconcave, expressed by the following equation.

$$\bar{y} = 0.5(1-\bar{x}^2)^{0.5}(c_0 + c_1\bar{x}^2 + c_2\bar{x}^4)$$
$$-1 \le \bar{x} \le 1;\ c_0 = 0.207, c_1 = 2.002, c_2 = 1.122 \quad (14)$$

In addition, these two circular models have been simulated to show the capability of the mentioned method due to their versatility. The process of deformation of different primary red blood cell geometries under shear flow (Table 1) is shown in Fig. 6. Also shown in Fig. 7 is the

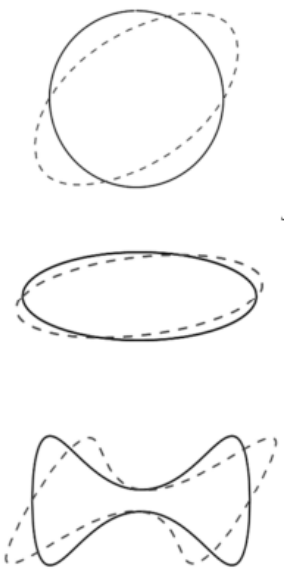

Figure 6: Red blood cells deformation with different geometries

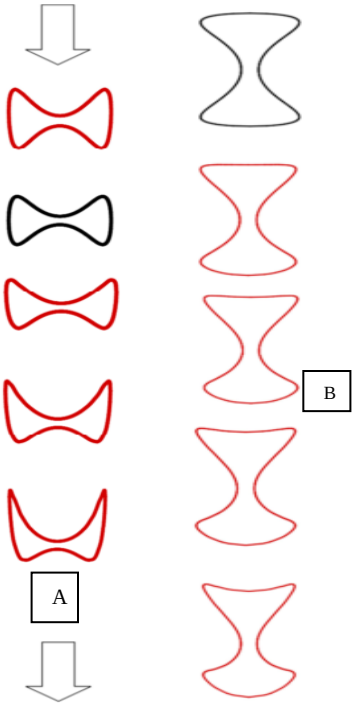

Figure 7: Deformation of red blood cells during movement in a canal

deformation associated with the displacement of a red blood cell in a canal. Fig. 7 shows the deformation and movement of a red blood cell in a channel with the initial geometry of two curves. The difference between Web Part A of this shape is in how the cell is positioned. As can be seen, in Fig. 6-a, the cell is located vertically in the flow path, while in Fig. 6-b, the red blood cell is placed horizontally in the flow path.

In the distal part, the flow inside a blood artery is analyzed to show the ability to simulate the flow in a bifurcated artery with complex geometry. Fig. 8a shows the geometry of the carotid artery as an example of a blood vessel with complex geometry. Fig. 8b shows the flow lines inside this blood vessel.

To ensure the accuracy of the results, the velocity profiles in the three identified sections were compared with the results reported by Steinhaven et al. [20] (Figure 1). As can be seen, the obtained velocity profiles have an acceptable agreement with the laboratory results.

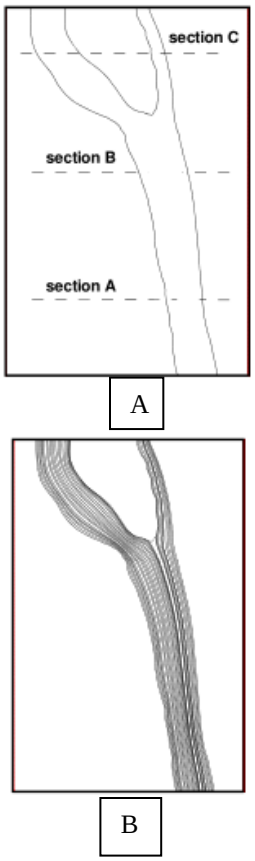

Figure 8: (a) Scheme and (b) flow lines in the carotid artery

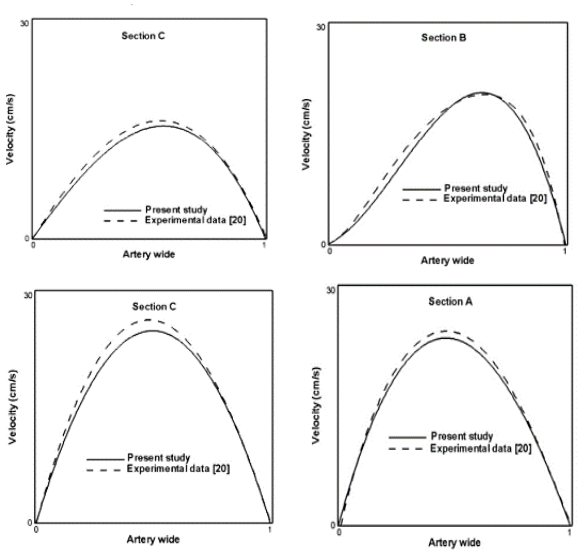

Figure 9: Velocity profiles at different sections in the carotid artery

As shown in Fig. 9, by moving from the bottom of the vessel to the branch, the maximum point of the velocity profile is gradually drawn towards the right branch. Also, in the final section, it is observed that the velocity profile in the left fork is flatter than the profile for the right fork. In this section, after confirming the accuracy of the simulation, how to block the blood artery and drug delivery is analyzed.

If blood flow to the blood vessels stops, the target tissue is destroyed by a lack of oxygen. If blood flow outside the body does not stop after serious injuries, a person will die from bleeding. However, the bleeding usually stops within minutes of the incision. Occasionally, blood can clot in blood vessels due to abnormal substances floating in the blood or tissue damage. Any deficiency in blood clotting control agents can increase or decrease the risk of blood clotting. In this section, arterial tissue damage is simulated in Fig. 10. Careful examination of this figure shows the effect of artery occlusion and its effect on blood flow. As can be seen, obstruction of the pathway causes circulatory flow and increases the likelihood of blood clotting or accumulation of adipose tissue in these areas. Drug delivery involves transferring a drug compound into the body to achieve the desired therapeutic effect. In this process, both the quantity and quality of the drugs needed by tissue are very important.

Fig. 11 shows the various spherical particles that

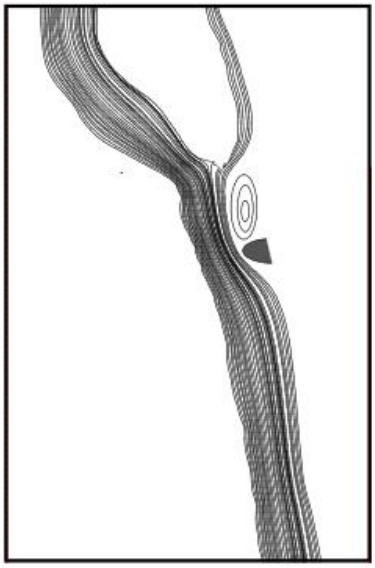

Figure 10: Flow lines in the state of carotid artery occlusion

are released from different arteries in different areas. These areas are shown in Fig. 8 (a), as it can be seen that the particles released in different areas have chosen different paths for themselves. A closer look at these results reveals that about 65% of the particles released before cutting A choose the right fork, and about 70% of the particles released between cutting A and B choose the left fork to continue their path. These results show that by controlling the injection site of the drug in this artery, the quantity of drug distribution between the two branches can be controlled.

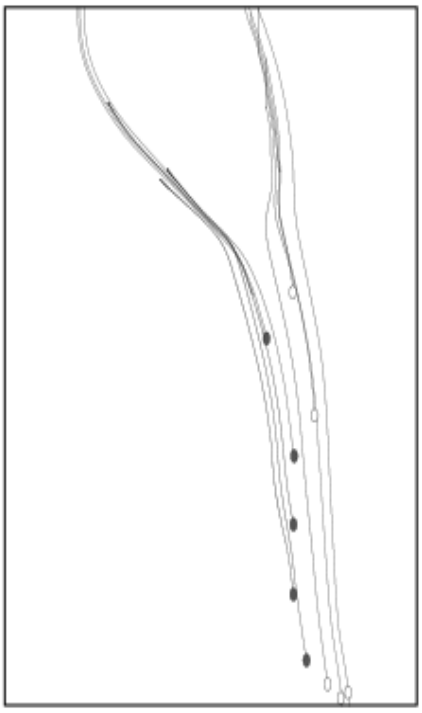

Figure 11: The path of the particles released in the carotid artery

Accurately predicting drug delivery is a critical task in drug development research and clinical trials [1,2]. It requires careful consideration of physiological conditions, such as hematocrit level (the volume ratio between red blood cell and the whole blood) [3,4], vessel geometry and flow conditions [5-7], drug carrier size and shape [3,8], dissolution rate [9] and external stimuli [10,11]. For small particles in red blood cell (RBC) suspensions, such as nanoparticles (NP) and platelets, as was mentioned in the aims of this paper, a new mathematical method is applied in this paper for simulation of this process which is aligned to the recent studies that have demonstrated that local flow field disturbances caused by RBC translation and deformation can enhance particle dispersion [3,12-16]. The migration of particles in RBC suspensions under shear has been shown to behave like a random walk process [17,18], with a dispersion rate much larger than thermal diffusion. Therefore, accurate predictions of NP dispersion in RBC suspensions must consider fluid-structure interaction between the immersed solid bodies (particles and cells) and the surrounding fluid. Previously-developed models for predicting NP dispersion in RBC suspensions have relied primarily on empirical data fitting. The method in this paper is aligned with Aarts et al. experimentally studied shear-induced platelet diffusivity (D), which was fitted with shear rate (η) as a power-law $D = k\eta^n$, where k is a constant and n is a function of hematocrit, and the results were close to ours [19]. However, the model parameters are obtained empirically rather than predicted from the underlying physics. Another similar research was Decuzzi et al. extended the Taylor–Aris theory to calculate an effective NP diffusion rate that considers wall permeability and blood rheology [20,21]. They also reported a three-fold increase in the dispersion rate of 1 μm compared to thermal diffusion [16]. Recently, Fedosov's group systematically studied micro-and nanoparticles in drug delivery, including particle size, shape effect, and RBC influence on particle margination and adhesion probabilities [3]. However, no analytical formula or quantitative rule directly predicts the NP dispersion rate so far, which is much needed in large-scale drug delivery simulations, a developed method of this study [20-26].

4 CONCLUSION

This study aimed to model the deformation of red blood cells and analyze how drugs are delivered and blocked in a blood vessel using the Boltzmann network method. Compared to conventional computational fluid dynamics methods, the Boltzmann network method can simulate complex problems with specific boundary conditions with a simple computational process. In this research, the flexibility of this

method has been evaluated by examining various parameters. The important conclusions are (1) Simulate the flow between two parallel plates, the most suitable comfort time is τ = 0.6. (2) Deformation of an elliptical cell obtained is in good agreement with the results reported by previous researchers. (3) Simulation of red blood cell deformation and movement with different geometries shows that this method has a high ability to analyze this type of problem. (4) Confirms the comparison of flow velocity profiles in the carotid artery with previous results. (5) Simulation results show that occlusion of blood vessels increases the likelihood of vortex flow of blood clots or accumulation of adipose tissue in these areas. (6) Analysis of drug delivery results indicates that the quantity of drug distribution between the two branches can be controlled by controlling the injection site.

ACKNOWLEDGEMENT

“Authors thanks Amirkabir university for their supports.”

REFERENCES

[1] C. S. Peskin. (1972). Flow patterns around heart valves: a digital computer method for solving the equations of motion. Yeshiva University.

[2] Y. Gao, Y. Yu, L. Yang, S. Qin, G. Hou. (2021). Development of a coupled simplified lattice Boltzmann method for thermal flows. Computers & Fluids.[in Press] 105042.

[3] N. Sokolovska, O. Permiakova, S.L. Forslund, J.D. Zucker. (2020). Using Unlabeled Data to Discover Bivariate Causality with Deep Restricted Boltzmann Machines. IEEE/ACM transactions on computational biology and bioinformatics. 17(1), pp. 358–364.

[4] C. Shu, Y. Peng, Y.T. Chew. (2002). Simulation of natural convection in a square cavity by Taylor series expansion-and least squares-based lattice Boltzmann method. International Journal of Modern Physics C. 13(10), pp. 1399-1414.

[5] A. D'Orazio, M. Corcione, G.P. Celata. (2004). Application to natural convection enclosed flows of a lattice Boltzmann BGK model coupled with a general purpose thermal boundary condition. International Journal of Thermal Sciences. 43(6), pp. 575-586.

[6] S.A. Urquiza, P.J. Blanco, M.J. Vénere, R.A. Feijóo. (2006). Multidimensional modelling for the carotid artery blood flow. Computer Methods in Applied Mechanics and Engineering. 195(33-36), pp. 4002-4017.

[7] C.Y. Chen, R. Antón, M.Y. Hung, P. Menon, E.A. Finol, K. Pekkan. (2014). Effects of intraluminal thrombus on patient-specific abdominal aortic aneurysm hemodynamics via stereoscopic particle image velocity and computational fluid dynamics modeling. Journal of biomechanical engineering. 136(3).

[8] Z. Guo, T.S. Zhao. (2002). Lattice Boltzmann model for incompressible flows through porous media. Physical review E. 66(3), 036304.

[9] R. Mei, D. Yu, W. Shyy, L.S. Luo. (2002). Force evaluation in the lattice Boltzmann method involving curved geometry. Physical Review E. 65(4), 041203.

[10] B. Chopard, P.O. Luthi. (1999). Lattice Boltzmann computations and applications to physics. Theoretical Computer Science. 217(1), pp. 115-130.

[11] R.R. Nourgaliev, T.N. Dinh, T.G. Theofanous, D. Joseph. (2003). The lattice Boltzmann equation method: theoretical interpretation, numerics and implications. International Journal of Multiphase Flow. 29(1), pp. 117-169.

[12] D. Yu, R. Mei, L.S. Luo, W. Shyy. (2003). Viscous flow computations with the method of lattice Boltzmann equation. Progress in Aerospace Sciences. 39(5), pp. 329-367.

[13] A.A. Mohamad. (2007). Applied lattice Boltzmann method for transport phenomena, momentum, heat and mass transfer. Canadian Journal of Chemical Engineering. 85(6), pp. 946-946.

[14] M.A. Delavar, M. Farhadi, K. Sedighi. (2009). Effect of the heater location on heat transfer and entropy generation in the cavity using the lattice Boltzmann method. Heat Transfer Research. 40(6).

[15] A. Mezrhab, M. Jami, C. Abid, M.H. Bouzidi, P. Lallemand. (2006). Lattice-Boltzmann modelling of natural convection in an inclined square enclosure with partitions attached to its cold wall. International journal of heat and fluid flow. 27(3), pp. 456-465.

[16] N. Thürey, U. Rüde. (2009). Stable free surface flows with the lattice Boltzmann method on adaptively coarsened grids. Computing and Visualization in Science. 12(5), pp. 247-263.

[17] F. Ramezani, M. Razmgir, K. Tanha, F. Nasirinezhad, A. Neshasteriz, A. Bahrami-Ahmadi, A. Janzadeh. (2020). Photobiomodulation for spinal cord injury: A systematic review and meta-analysis. Physiology & Behavior, 112977.

[18] M. Tashakori-Miyanroudi, K. Rakhshan, M. Ramez, S. Asgarian, A. Janzadeh, Y. Azizi, F. Ramezani. (2020). Conductive carbon nanofibers incorporated into collagen bio-scaffold assists myocardial injury repair. International Journal of Biological Macromolecules. 163, pp. 1136-1146.

[19] M. Vahed, F. Ramezani, V. Tafakori, V.S. Mirbagheri, A. Najafi, G. Ahmadian. (2020). Molecular dynamics simulation and experimental study of the surface-display of SPA protein via Lpp-OmpA system for screening of IgG. AMB Express. 10(1), pp. 1-9.

[20] P. Bagchi, P.C. Johnson, A.S. Popel. (2005). Computational fluid dynamic simulation of aggregation of deformable cells in a shear flow. Journal of biomechanical engineering. 127(7), pp. 1070-1080.

[21] A.A. Van Steenhoven, F.N. Van de Vosse, C.C. Rindt, J.D. Janssen, R.S. Reneman. (1990). Experimental and numerical analysis of carotid artery blood flow. Monogr. Atheroscler. 15, pp. 250-260.

[22] P.A. Aarts, P. Steendijk, J.J. Sixma, R.M. Heethaar. (1986). Fluid shear as a possible mechanism for platelet diffusivity in flowing blood. Journal of biomechanics. 19(10), pp. 799-805.

[23] F. Gentile, M. Ferrari, P. Decuzzi. (2008). The transport of nanoparticles in blood vessels: the effect of vessel permeability and blood rheology. Annals of biomedical engineering. 36(2), pp. 254-261.

[24] E.O. Kung, A.S. Les, F. Medina, R.B. Wicker, M.V. McConnell, C.A. Taylor. (2011). In vitro validation of finite-element model of AAA hemodynamics incorporating realistic outlet boundary conditions. Journal of biomechanical engineering. 133(4).
[25] B. Mondal, S. C. Mishra. (2008). Simulation of natural convection in the presence of volumetric radiation using the lattice Boltzmann method. Numerical Heat Transfer, Part A: Applications. 55(1), pp. 18-41.
[26] M.A. Mussa, S. Abdullah, C.N. Azwadi, N. Muhamad. (2011). Simulation of natural convection heat transfer in an enclosure by the lattice-Boltzmann method. Computers & Fluids. 44(1), pp. 162-168.